

Optyx: A ZX-based Python library for networked quantum architectures

Mateusz Kupper^{1,2}, Richie Yeung^{1,3}, Boldizsár Poór^{1,3}, Alexis Toumi⁴, William Cashman³, and Giovanni de Felice¹

¹Quantinuum, 17 Beaumont Street, Oxford, OX1 2NA, United Kingdom

²University of Sussex, United Kingdom

³University of Oxford, United Kingdom

⁴DisCoPy, France

Distributed, large-scale quantum computing will need architectures that combine matter-based qubits with photonic links, but today’s software stacks target either gate-based chips or linear-optical devices in isolation. We introduce `Optyx`, an open-source Python framework offering a unified language to program, simulate, and prototype hybrid, networked systems: users create experiments that mix qubit registers, discrete-variable photonic modes, lossy channels, heralded measurements, and real-time feedback; `Optyx` compiles them via ZX/ZW calculus into optimised tensor-network forms, and executes with state-of-the-art contraction schedulers based on `Quimb` and `Cotengra`. Benchmarking on exact multi-photon circuit simulations shows that, versus permanent-based methods, tensor network contraction can deliver speedups of orders of magnitude for low-depth circuits and entangled photon sources, and natively supports loss and distinguishability – establishing it as both a high-performance simulator and a rapid-prototyping environment for next-generation photonic-network experiments.

1 Introduction

The promise of universal, fault-tolerant quantum computation is intimately tied to our ability to scale beyond the confines of a single, monolithic chip. Networked and modular architectures – in which physically distinct quantum

Mateusz Kupper: mateusz.kupper@quantinuum.com

nodes are coherently linked by photonic interconnects – are emerging as a compelling path to scalability [1]. By decoupling the generation, processing, and storage of quantum information, these hybrid platforms leverage the long-range, room-temperature propagation of photons to mediate entanglement between otherwise monolithic hardware, from superconducting qubits to trapped ions and neutral atoms. Recent demonstrations of remote Bell pairs [1, 2, 3, 4], reconfigurable photonic routers [1, 2], and metropolitan-scale quantum key distribution [5] highlight the rapid experimental progress. Yet translating these advances into practical, large-scale applications demands software abstractions that can express the concurrent, distributed, and multi-modal nature of networked experiments.

Current quantum programming frameworks remain largely committed to a circuit paradigm that assumes a single register of qubits evolving under a sequence of unitary gates and computational-basis measurements. Toolkits such as `Qiskit` [6], `Cirq` [7], `tket` [8], excel at describing gate-based processors, but offer only rudimentary support for different modes of computation such as with light-matter interaction. Conversely, photonic-native simulators focus on either Gaussian (continuous-variable) photonic computing (`Strawberry Fields` [9], `The Walrus` [10]), bosonic discrete-variable modes and permanent-based sub-routines for simulation (`Perceval` [11], `SOQCS` [12], `Linopt` [13]), or hybrid continuous-variable and discrete-variable photonics or general quantum mechanics (`Piquasso` [14], `Mr Mustard` [15], `QuTiP` [16], `QuantumOptics.jl` [17]). The Python package `GraphiQ` [18] is designed to produce quantum circuits that generate specific photonic graph states,

while **Graphix** [19] provides tools for generating, optimising, and simulating measurement patterns in measurement-based quantum computing. Therefore, the existing software lacks facilities for integrating qubits, real-time feedback, or a high-level description of network topologies. In short, no existing platform offers a unified language for programming all the components of a distributed, heterogeneous architecture.

String-diagrammatic calculi such as *ZX* and *ZW* provide a typed, compositional representation for quantum circuits and channels, with a small set of sound rewrite rules that support semantics-preserving optimisation – compiling via *ZX* enables graph-theoretic simplifications (local complementation, pivoting) and reliable circuit extraction [20], yielding depth and gate-count reductions and, in the fault-tolerant regime, substantial *T*-count savings via phase teleportation [21, 22]. *ZX*-calculus can also be used to check the equivalence of quantum circuits [23, 24]. Mature tooling further makes these calculi attractive for software development: **PyZX** (and its Rust port **QuiZX**) implements large-scale automated rewriting and validation workflows [25]. **DisCoPy** [26] provides a Pythonic framework for constructing and reasoning about string diagrams, supporting the definition of custom categories and functors, including user-defined interpretations to concrete semantics such as tensor networks.

Tensor-network (TN) methods have emerged as a powerful bridge between high-level circuit descriptions and low-level, hardware-specific simulations. By exploiting entanglement structure, TNs routinely push the classical simulability frontier of qubit circuits, and have been extended to Gaussian boson sampling [27, 28], spin-boson dynamics [29], optical circuits [30] and open-system modelling [31]. The application of TNs to *multi-node photonic networks* remains in its infancy: existing methods either restrict to linear-optical interferometers or require manual construction of the network graph, and none provide an end-to-end workflow from syntax to numerics.

This paper introduces **Optyx**¹, an open-source Python package that fills this gap. The package is an implementation of the dataflow programming framework for linear optical distributed quan-

tum computing [32]. Building on the categorical quantum mechanics ecosystem (**DisCoPy**, **PyZX**), **Optyx** offers a compositional domain-specific language in which gates, measurements, states, and quantum channels can be wired together into *string diagrams*. These diagrams are compiled automatically into *ZX/ZW* fragments and subsequently into optimised tensor-network contractions using **Cotengra** and **Quimb**. The result is a simulator that (i) supports both qubit and discrete-variable photonic modes in a common formalism, (ii) transparently handles classical control, mid-circuit feedback, and probabilistic branching, and (iii) exposes differentiable backends for gradient-based design and calibration of hybrid experiments.

Beyond numerical simulation, we position **Optyx** as a *prototyping environment* for networked quantum optics. Users may encapsulate sub-circuits as reusable components, assemble them into layered architectures connected by ideal or lossy channels, and deploy the same description to either an exact or approximate TN backend or (in the future) on hardware.

In the remainder of this article we: (i) give an overview of the software: basic syntax and evaluation methods (§2); (ii) present the core building blocks provided by **Optyx** (§3); (iii) discuss how to model noise and errors (§4); (iv) describe conversion of circuits to and from other software (§5); (v) detail the translation from diagrams to optimised tensor networks (§6); and (vi) demonstrate the capabilities of the framework on three representative use cases: simulation of photonic observables with entangled states, distributed entanglement generation, and variational optimisation (§7).

2 Overview

Our library provides a diagrammatic toolkit for prototyping and simulating hybrid quantum architectures. It exposes:

1. a **functional front-end** (Pythonic, compositional),
2. a compact **intermediate representation** for *ZX/ZW* generators with classical control, and
3. pluggable **backends** (e.g., exact, tensor-network, permanent-based) for evaluation

¹Source code available at <https://github.com/quantinuum-dev/optyx>.

and **converters** for importing/exporting circuits from/to external tools.

Basic syntax The circuits in **Optyx** (which we call *diagrams* following the convention from the string diagram literature) are composed of generators representing quantum channels (CPTP maps). Because the composition rules allow for mixing classical and quantum wires, users can freely interleave them, routing classical measurement results into photonic or qubit feed-forward corrections, embedding qubits in photonic interferometers by using the dual-rail encoding where logical states are encoded in the single-photon subspace of two modes [33], or calling classical post-processing routines without leaving the tensor-network formalism which provides the semantics for all circuits in **Optyx**. Hybrid circuits are therefore *first-class citizens* that compile, optimise, and execute through the very same tensor-network-based backend.

In **Optyx**, boxes represent maps, wiring boxes in series denotes sequential composition, and placing them side by side denotes the monoidal (parallel) product. Concretely, we follow the **DisCoPy** style: a *diagram* is a typed compositional object. A map $f : A \rightarrow B$ can be composed in parallel (tensored) with $g : C \rightarrow D$ to obtain $f \otimes g : A \otimes C \rightarrow B \otimes D$, or composed in sequence when codomain and domain coincide; in code we write `@` and `>>` respectively. The same high-level diagram can later be interpreted as a tensor network, or a permanent computation. Four primitive system types appear throughout: `bit` for classical two-level data, `mode` for classical natural numbers (e.g. photon counts), `qubit` for two-dimensional quantum systems, and `qmode` for discrete-variable photonic modes. Qubit sub-diagrams are mostly expressed in the ZX-calculus, whose green (Z) and red (X) spiders form two interacting commutative Frobenius algebras [34]; the related ZW-calculus is convenient for infinite-dimensional discrete Hilbert spaces and features Z spiders, the binomial split/merge maps (the W nodes), and photon creations and selections [35]. **Optyx** uses ZX/ZW diagrams to enable a conversion to tensor networks.

Function syntax The example of teleportation (see Code Listing 1) showcases both sequen-

tial (`>`) and parallel composition (`@`) to build a hybrid protocol. Alternatively, we can use the *function syntax* instead of manual composition using `>`. In this case, the generators act as functions defined on their domain wires. This approach is particularly useful when a diagram would otherwise require the user to manually insert `Swap` boxes to reorder wires. Since the wires are labelled using function syntax, the user can directly reference these labels as inputs to the appropriate boxes. The function syntax is similar to how the quantum programs are defined in **Guppy** [36]. We provide an example of both the monoidal and function syntax in Code Listing 1.

Evaluation with backends Numerical simulation proceeds by translating diagrams to tensor networks: each generator becomes a tensor, each wire an index, and diagram composition becomes index contraction. The difficulty of simulation is governed by the contraction order (path) and intermediate tensor sizes. **Optyx** compiles diagrams by (i) converting them to tensor networks, and (ii) handing the resulting TN to **Cotengra** for path optimisation and to **Quimb** for contraction (CPU/GPU, dense/sparse). TNs scale well when circuits have low treewidth and shallow depth; they fail sharply when intermediate tensors exceed memory.

For purely linear-optical amplitudes the standard alternative is permanent-based simulation: for an $m \times m$ interferometer U acting on an n -photon Fock input $|\mathbf{s}\rangle$ (with $\sum_i s_i = n$), the amplitude for outcome $|\mathbf{t}\rangle$ is,

$$\langle \mathbf{t} | U | \mathbf{s} \rangle = \frac{\text{Perm}(U_{\mathbf{t}, \mathbf{s}})}{\sqrt{\prod_i s_i! \prod_j t_j!}}, \quad (1)$$

where $U_{\mathbf{t}, \mathbf{s}}$ repeats rows/columns according to occupations. Computing the permanent is $\#P$ -hard [37], with best-known exact algorithms scaling like $O(2^n n)$ (e.g., Ryser [38], Glynn [39] algorithms). For approximate permanent calculation, Gurvits' algorithm gives an additive estimate of a permanent: for an $n \times n$ matrix A it computes $\text{Per}(A)$ within $\pm \varepsilon \|A\|^n$ in $O(n^2/\varepsilon^2)$ time; because linear-optical output amplitudes are permanents of unitary submatrices, this yields efficient additive approximations to *individual photonic outcome probabilities* [40]. Toolkits such as **Perceval** [11] provide permanent-based evaluators, **SLOS** [41], and Gurvits' which are advan-

Module	Description
<code>optyx.channel</code>	Wire swaps; identity channels; discarding, measurement and preparation
<code>optyx.qubits</code>	ZX gates; imported external circuits; qubit errors
<code>optyx.photonic</code>	Linear-optical & dual-rail operators; photon sources; detectors
<code>optyx.classical</code>	Boolean logic; \mathbb{N} arithmetic; post-selection; control boxes

Table 1: The main sub-modules of `Optyx` and their functionality.

tageous when only a few amplitudes are needed or when n is small. Consequently, permanent-based methods excel for typical low-width passive linear-optical circuits, whereas adding active control and feed-forward, non-unitaries, or hybrid qubit-photon models quickly becomes cumbersome for permanent-based approaches (with these setups the number of permanents to calculate can scale exponentially). By contrast, the tensor-network methods we describe in this article natively handle these features. `Optyx` exposes both TN and permanent-based backends.

Diagrams can be evaluated using the `Quimb` backend (exact or approximate evaluation), the `Perceval` backend² (with permanent-based algorithms), or the `DisCoPy` backend. By default, evaluation is performed with `Quimb` exact contraction: `result = circ.eval()`. The `result` object provides ways to obtain amplitudes of the resulting state, probability distribution, or a density matrix.

Example: qubit teleportation Quantum teleportation uses classical and quantum data (it is therefore a *classical-quantum ZX diagram*). In `Optyx`, we can make use of controlled boxes from `optyx.classical` to correct the state of the qubit depending on the measurement result (see Figure 1).

```

1 @Channel.from_callable(
2     dom=qubit @ qubit, cod=qubit @ qubit
3 )
4 def cnot(a, b):
5     c, d = Z(1, 2)(a)
6     Scalar(2 ** 0.5)()
7     return c, X(2, 1)(d, b)
8
9 bell = Scalar(0.5 ** 0.5) @ Z(0, 2)
10
11 @Channel.from_callable(
12     dom=qubit, cod=qubit
13 )

```

²Note that currently only linear optical channels can be evaluated using this method.

```

14 def teleportation(c):
15     a, b = bell()
16     cc, aa = cnot(c, a)
17     c_ = Measure(1)(H()(cc))
18     a_ = Measure(1)(aa)
19     bb = CtrlX(a_, b)
20     return CtrlZ(c_, bb)
21
22 teleportation_monoidal_syntax = (
23     qubit @ bell >>
24     cnot @ qubit >>
25     H() @ qubit ** 2 >>
26     Measure(1) @ Measure(1) @ qubit >>
27     bit @ CtrlX >>
28     CtrlZ
29 )

```

Code Listing 1: Teleportation protocol with classical control using both monoidal and function syntax.

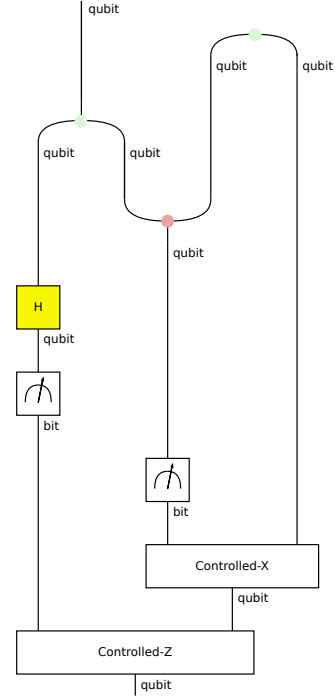


Figure 1: Diagram of the teleportation protocol in ZX-calculus. We discuss quantum teleportation using fusion measurements in the Appendix B.

In the following sections, we discuss the main building blocks of `Optyx` in more detail: the

`qubits` and `photonic` modules. Many examples make use of the `classical` module to perform classical operations on the results of quantum measurements, such as post-selection, copying, or discarding bits.

3 Building blocks

We have three kinds of generators: `qubits` generators, `photonic` generators, and `classical` generators (see Table 1). Intuitively, they represent gates and transformations on appropriate types. The generators make use of the following types: `bit` and `mode` for classical information (bit and natural number arithmetic respectively), and `qubit` and `qmode` for quantum degrees of freedom (qubit and photonic (Fock space) types). At the end of this section (see Subsection 3.5), we also discuss the stream processes which allow us to build synchronous circuits with feedback loops and delays and execute them for a specified number of time-steps.

3.1 General channels

There are generators in `Optyx` which belong to all the classes (`qubits`, `photonic`, and `classical`) and their specific use depends on the types supplied.

Channel class The superclass of all generators in `Optyx`. It can be used to define custom channels (maps) in `Optyx`. It is achieved by supplying a Kraus map to a `Channel` (see Appendix A) together with the types for the domain and codomain.

Classical-quantum generators These are the generators which interface between classical types (`bit` and `mode`) and quantum types (`qubit` and `qmode`):

- `Discard(type)`: discards a wire of type `type`. For example, we can use this to trace out qubit registers.
- `Measure(type)`: by measuring a quantum type, we obtain a corresponding classical register ($\text{qubit}^{\otimes m} \rightarrow \text{bit}^{\otimes m}$ and $\text{qmode}^{\otimes m} \rightarrow \text{mode}^{\otimes m}$).

- `Encode(type)`: the reverse of `Measure(type)` - we can use this to encode classical data in quantum registers (state preparation).

We also have other generators, which do not fall into the qubit, photonic or classical categories and require data types to be specified. These are `Id`, `Swap`, `Scalar`, `Spider`, and `Copy`. For example `Id(mode**2 @ qubit)` is an identity operator on two modes and one qubit.

3.2 Qubit primitives

The sub-module `optyx.qubits` collects every generator that acts on qubit registers: ZX-calculus generators, wrappers around circuit descriptions from external sources, basis preparations and measurements, and a handful of noise models (see Table 2). As other external packages (like `tket` or `Graphix`) offer well-established circuit or measurement pattern descriptions, we provide a way to wrap these objects into the `Optyx` framework, while also maintaining a basic set of generators that can be used to construct circuits from scratch directly in `Optyx`.

The main way of defining qubit maps in `Optyx` is using ZX diagrams. In particular, we are interested in using them to represent, for example, graph states for measurement-based quantum computing (MBQC) [42] or fusion-based computing [43]. We include the usual generators of ZX-calculus such as `Z`, `X`, and `H`, which can be imported from both `optyx.classical` and `optyx.qubits`. The classical versions act on `bit` types, while the quantum versions act on `qubit` types. For example, `X(1, 1, 0.5)` imported from `optyx.classical` represents a classical NOT gate, whereas the same gate imported from `optyx.qubits` corresponds to a Pauli-X gate acting on a qubit.

Since we are dealing with mixed channels, we also include generators that interface between classical and quantum systems: `Encode` (encoding a classical `bit` into a `qubit`), `Measure` (measuring a qubit in the computational basis to obtain a `bit`), and `Discard` (tracing out a qubit or deleting a `bit`). Using these, one can build *classical-quantum ZX diagrams* that mix quantum ($\text{qubit}^{\otimes m} \rightarrow \text{qubit}^{\otimes n}$) and classical ($\text{bit}^{\otimes m} \rightarrow \text{bit}^{\otimes n}$) components within a single diagram.

Table 2: Summary of available qubit primitives

Category	Primitives	Description
Circuits	<code>Circuit</code> , <code>QubitChannel</code>	Quantum circuits and channels operating on qubits.
ZX	<code>Z</code> , <code>X</code> , <code>H</code> , <code>Scalar</code> , <code>Bra</code> , <code>Ket</code>	Core ZX-calculus generators (spiders, Hadamard, scalar).
Errors	<code>BitFlipError</code> , <code>DephasingError</code>	Stochastic error channels acting on qubits.

3.3 Photonic primitives

Discrete-variable modes are implemented in `optyx.photonic`. The module organises its generators into five categories summarised in Table 3: measurements, linear-optical gates, dual-rail operators, states, and utility channels. Below each category is described in more detail.

Linear-optical gates All passive linear optical gates support `.dagger()` and `.conjugate()`, accept symbolic parameters, and are differentiable.

- `BBS(bias)` – biased beam-splitter, balanced when `bias = 0`; reproduces the Hong-Ou-Mandel dip [44].
- `TBS(phi)` – continuously tunable beam-splitter with mixing angle θ .
- `MZI(psi,phi)` – two-phase Mach-Zehnder interferometer.
- `Phase(psi)` – single-mode phase shift

Measurements In `Optyx`, we provide two types of photonic measurements:

- `PhotonThresholdMeasurement` – a click/no-click detector that returns a single classical bit (1 if at least one photon is present).
- `NumberResolvingMeasurement(n)` – resolves the full photon-count pattern on n modes and outputs `mode $^{\otimes n}$` .

Photon sources - dual-rail and Fock states

The `Create` generator prepares Fock states on n modes. It accepts a list of occupations and an optional list of internal states (to model photon distinguishability, see Section 4). Likewise, `DualRail` encodes a qubit into two photonic modes using a single photon. It also optionally accepts a list of internal states (internal degrees of

freedom for circuits with varying degrees of photon distinguishability, see Section 4).

3.4 Classical layer and hybrid control

The `optyx.classical` module supplies logic, arithmetic on natural-number modes, and control boxes that condition quantum sub-circuits on classical data (see Table 4). The generators are organised in two categories: primitives for classical computations (obtainable from explicit generators - logical gates and arithmetic on modes, Python functions³ and Boolean matrices), and primitives acting on quantum types (`qubit` and `qmode`) that condition quantum gates on classical data (e.g. `BitControlledGate`). Hybrid control is obtained with `BitControlledGate` and `BitControlledPhaseShift`.

Taken together, these generators let users script algorithms, graph states, realistic error channels, and hybrid qubit-photon experiments - *all* within a single tensor-network semantics that compiles to either `Quimb` contractions or permanent-based linear-optical paths as required.

3.5 Feedback and delay

Modern optical setups with sources, routers, and delay lines require us to reason about how systems evolve over many time-steps with feedback. Stream processes are diagrams for such time-extended behaviours: they describe (potentially infinite) sequences of inputs and outputs and provide a language to analyse and transform realistic optical circuits. For a formal definition of streams, see Ref. [32], Section 4.

³To obtain a tensor for a given Python function, `Optyx` evaluates the function on all possible inputs for given input dimensions and constructs a tensor with the corresponding output values.

Table 3: Summary of available photonic primitives

Category	Primitives	Description
Linear optical gates	Gate, Phase, BBS, TBS, MZI, ansatz	Unitary transformations built from beam splitters, phase shifters, and general interferometers.
Dual-rail operators	DualRail, HadamardBS, PhaseShiftDR, ZMeasurementDR, XMeasurementDR, FusionTypeI, FusionTypeII	Gates and measurements for qubits encoded in dual-rail photonic modes.
Measurements	PhotonThresholdMeasurement, NumberResolvingMeasurement	Operations that measure photon number.
States	Create	Preparation of bosonic product states.
Other	NumOp, PhotonLoss	Miscellaneous operators.

Table 4: Summary of available *classical* primitives

Category	Primitives	Description
Logic gates	Not, Xor, And, Or, Z, X	Boolean operations and ZX spiders acting on classical bits.
Arithmetic on modes	Add, Sub, Multiply, Divide, Mod2	Integer arithmetic and data-movement primitives on natural-number modes.
Control & feedforward	BitControlledGate, BitControlledPhaseShift, CtrlX, CtrlZ, ClassicalFunction, BinaryMatrix	Classical control of quantum gates and generic functions/matrix maps on bit or mode registers.

Informally, a stream process from an input stream X to an output stream Y is a circuit executed repeatedly in discrete time-steps, together with an internal memory carried from one step to the next. At time-step 0 the process takes X_0 and an initial memory M_0 , produces Y_0 , and updates the memory to M_1 . From time-step 1 onwards, the same pattern repeats with (X_i, M_i) producing (Y_i, M_{i+1}) . Unfolding this recursion, a stream is determined by its family of one-step maps

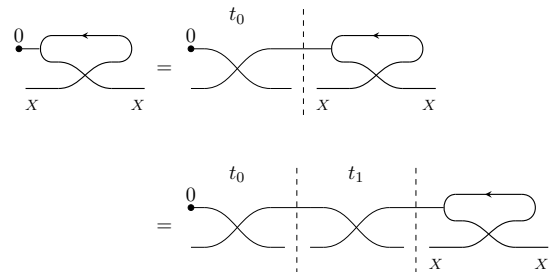
$$f_i : M_i \otimes X_i \rightarrow M_{i+1} \otimes Y_i \quad (i = 0, 1, 2, \dots),$$

where M_i is the memory linking time-steps.

In this setting, feedback is the operation that creates and updates this memory: it takes a process with an extra input/output system S and connects those wires in a loop, so that the value of S produced at one time-step is stored and later fed back as an input. Physically, this corresponds to sending part of the signal through a delay line or quantum memory and re-injecting it into the

setup.

A basic example built from feedback is a delay. To implement a delay we use a stream of length 1 on X that takes the current value at time-step i , stores it in memory, and outputs instead the value stored at time-step $i - 1$. Diagrammatically, this is obtained from a suitable feedback of a swap:



A delay of length d is given by composing d unit delays, so that each value remains in memory for d time-steps before being output. The delay can be implemented in Optyx as in Code Listing 2.

```
1 from optyx import Diagram, qmode
2 from optyx.photonic import Create
```

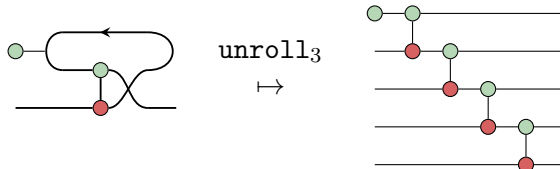
```

3 Diagram.delay(
4   ty=qmode,
5   initial_state=Create(0)
6 )
7 )

```

Code Listing 2: Delay on a `qmode` with an empty initial state.

Other processes can also be modelled with feedback – consider unrolling of a CNOT ladder:



We can implement this exact stream in `Optyx` like in Code Listing 3. Here `diagram` defines the one-step body of the process; the call `diagram.feedback(dom=..., cod=..., mem=..., initial_state=...)` applies the feedback construction, turning this body into a stream by introducing a single-qubit memory wire that is threaded between time-steps; and the final call to `.unroll(3)` materialises the first three time-steps of this infinite stream as a finite diagram.

```

1 diagram = (
2   X(1, 2) @ qubit >>
3   qubit @ Z(2, 1) >>
4   Swap(qubit, qubit)
5 )
6
7 diagram.feedback(
8   dom=qubit,
9   cod=qubit,
10  mem=qubit,
11  initial_state=Z(0, 1)
12 ).unroll(3)

```

Code Listing 3: CNOT ladder stream process.

4 Noise and errors

Photon distinguishability Nanosecond timing slips, energy shifts, or polarisation changes let two photons be told apart. This source of errors is called photon distinguishability. In photonic quantum computers this spoils the bosonic interference that most gates need, boosting mis-fires and error rates. Keeping photons indistinguishable is therefore as vital as low loss and high detector efficiency for scalable photonic processors. We model distinguishability in `Optyx` (see the example Code Listing 5) by assigning *internal states*

to photon sources (in `Create` and `DualRail` instances). The pairwise inner products between internal states from different sources define the S matrix of Ref. [45].

Photon loss It is the disappearance of a photon through absorption, scattering, imperfect coupling, or detector inefficiency before it can participate in its intended operation. Because each photonic qubit exists in just one photon (in dual-rail encoding), losing that photon erases the quantum state entirely, so circuit success probabilities plummet as systems grow and errors accumulate. As photon-loss is the leading source of error in current photonic systems, it is important to be able to model it. In `Optyx`, we provide the `PhotonLoss` generator to model photon loss (see the example Code Listing 6). It accepts a transmission probability $p \in [0, 1]$ and acts on `qmode` types. We are therefore able to model *non-uniform* photon loss [46] by placing `PhotonLoss` boxes with different p values in different locations.

Together, these primitives allow users to script anything from a single Hong-Ou-Mandel benchmark to a loss-tolerant dual-rail cluster-state factory, without leaving the tensor-network backend that powers `Optyx`.

Qubit errors We model single-qubit noise with two qubit generators. Two standard choices are the *bit-flip* channel and the *dephasing* (phase-flip) channel. For error probability $p \in [0, 1]$, they act on a qubit state ρ as

$$\mathcal{E}_{X,p}(\rho) = (1 - p) \rho + p X \rho X,$$

$$\mathcal{E}_{Z,p}(\rho) = (1 - p) \rho + p Z \rho Z.$$

In `Optyx`, these are provided as `BitFlipError(p)` and `DephasingError(p)` which act on the `qubit` type. They are used by inserting them *where the noise occurs*: after a gate to model control errors, before a measurement to model readout noise, or around a subroutine to model a noisy block.

Other (custom) noise channels can be defined by a user by defining their own channel (see Appendix A for an explanation of how to define a custom channel).

Example: the Hong-Ou-Mandel effect
The effect arises when two indistinguishable photons strike opposite inputs of a 50:50 beamsplitter

at the same moment; quantum interference drives them out through the same port, wiping out coincidence counts. The depth of this “HOM dip” measures indistinguishability, so a reduced dip flags timing, spectral, or polarisation mismatches that would lower photonic-gate fidelity. Let us consider the following example of a HOM dip with perfectly indistinguishable photons in Code Listing 4. The probability of detecting one photon in each output mode is 0.0, while the probability of detecting both photons in one of the output modes is 0.5, which is the expected value for a perfectly indistinguishable pair of photons.

```

1 from optyx.photonic import BS, Create
2
3 beam_splitter = BS
4
5 HOM = (
6     Create(1) @ Create(1) >>
7     beam_splitter
8 )
9
10 assert np.allclose(
11     HOM.eval().prob_dist()[1, 1], 0.0
12 )

```

Code Listing 4: Hong-Ou-Mandel effect with two indistinguishable photons.

In Code Listing 5, the two internal states are random array-like vectors of unit norm: s_1 and s_2 . `Create` can accept internal states of photons as an argument. `Channel.inflate` is used to indicate evaluation of the channel taking into account the internal states. The probability of detecting one photon in each output mode should be $\frac{1}{2} - \frac{1}{2} \langle s_1 | s_2 \rangle$.

```

1 import numpy as np
2 from optyx.photonic import BS
3
4 s_1 = [1, 0]
5 s_2 = [np.sqrt(0.9), np.sqrt(0.1)]
6
7 create = Create(1, 1, internal_states=(s_1, s_2))
8
9 distinguishable_HOM = (
10     create >> BS >>
11     NumberResolvingMeasurement(2)
12 )
13
14 result = distinguishable_HOM.inflate(
15     len(s_1)).eval().prob_dist()
16
17 theoretical_result = 0.5 - 0.5 * np.abs(
18     np.array(s_1).dot(
19         np.array(s_2).conjugate()))**2
20 assert np.isclose(result[(1, 1)],

```

```
theoretical_result, 3)
```

Code Listing 5: Hong-Ou-Mandel effect with two distinguishable photons.

With photon loss, the HOM effect does not hold anymore. We can actually observe one photon in one output mode with a non-zero probability. In Code Listing 6 we model photon loss using the `PhotonLoss` generator. If we lose one of the two photons with probability 0.2, then the probability of detecting one photon overall is also 0.2.

```

1 lossy_HOM = (
2     Create(1, 1) >>
3     PhotonLoss(0.8) @ Id(1) >>
4     BS >>
5     NumberResolvingMeasurement(2) >>
6     Add(2)
7 )
8 assert np.isclose(
9     lossy_HOM.eval().prob_dist()[(1,)],
10     0.2
11 )

```

Code Listing 6: An example demonstrating photon loss. If we create two photons in two modes and lose one of them with probability 0.2, then the probability of detecting one photon overall is 0.2.

5 External interfaces

Converting external qubit circuits A complete circuit or measurement pattern created in `tket`, `PyZX`, `Graphix`, or `DisCoPy` becomes a single channel with one line of code which can then be composed with other `Optyx` diagrams and evaluated using `Optyx`’s backends.

Any `ZX` diagram in `PyZX` can be translated into a `Diagram` using the method `from_pyzx()` (this results only in pure diagrams). Quantum circuits defined in `tket`, or `DisCoPy` can also be converted into `Optyx` circuits (both pure and mixed).

A measurement pattern from `Graphix` [19] can also be converted into an `Optyx` circuit. For example, we can define a circuit in `Graphix`, transpile it into a measurement pattern and then convert its underlying graph into an `Optyx` circuit.

Converting external photonic circuits We can convert photonic circuits from `Perceval` [11] into `Optyx`; for example, one can define a teleportation circuit with feed-forward in `Perceval` and then translate it into an equivalent `Optyx`

circuit. While the converter does not support every `Perceval` feature (e.g. time delays), we can convert any circuit or processor that can be represented as a linear-optical circuit with feed-forward, including measurements, heralding, and post-selection.

6 Construction and evaluation of tensor networks

In `Optyx`, diagrams are the level of syntax, while tensor networks provide the operational semantics. The overall workflow is as follows: a user builds a diagram; a functorial translation turns that diagram into a tensor network; an optimiser finds an inexpensive contraction order; and an execution backend carries out the contractions numerically.

6.1 From a diagram to a tensor network

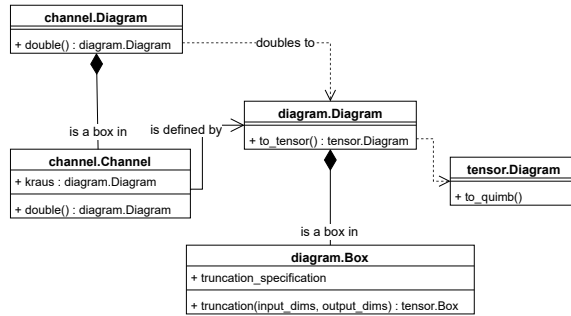


Figure 2: A UML class diagram [47] of the tensor-conversion logic: channels depend on diagrams for the definition of their Kraus maps, during evaluation these Kraus maps are used to construct a tensor network by doubling the Kraus maps and converting them to tensors.

The package builds on `DisCoPy` [26]. Channel diagrams are built from instances of `channel.Box`, each initialised by a Kraus map within a `diagram.Diagram`. The interpretation of every `channel.Diagram` is obtained by constructing the completely positive map induced by the Kraus operators of each box and their conjugates, a process known as *doubling* [48]. This procedure yields an instance of `diagram.Diagram` from each `channel.Diagram`.

Every generator in `diagram.Diagram` is itself an instance of `diagram.Box` (for example, the ZX or ZW generators), equipped with

a method `truncation()` that defines the corresponding tensor by its action on basis vectors. The resulting `diagram.Diagram` can then be converted into a `disco.tensor.Diagram` via `to_tensor()`, and further into a `Quimb` tensor network using `to_quimb()`. To obtain tensors of minimal dimension, an instance of `core.diagram.Diagram` is scanned from inputs to outputs so that the appropriate dimensions can be supplied to `truncation` when constructing the tensor network. This is achieved by creating “light-cones” for each generator to determine the number of photons which can reach it from the inputs.

The backend workflow is thus:

1. The user builds a channel diagram using generators from `photonic`, `qubits`, and `classical`.
2. Calling `double()` on the channel diagram produces a doubled `core.diagram.Diagram` assembled from the Kraus maps. This is the *CQ interpretation (doubling)* of the original diagram (see Figure 3).
3. The doubled diagram is composed of ZX and ZW generators.
4. Calling `to_tensor()` on this diagram converts it into a `DisCoPy` tensor diagram.
 - Each generator is turned into a tensor by invoking its `truncation` method, which returns a tensor with the computed minimal dimensions.
5. The `DisCoPy` tensor diagram is translated into a `Quimb` tensor network.
6. The resulting tensor network is ready for optimisation and execution.

6.2 Choosing and executing a contraction

Once the tensors are built, their pattern of shared indices defines a tensor network. The resulting TN is passed to `Cotengra`’s optimiser, which explores contraction trees and optionally slices indices to respect a memory cap. Slicing fixes the values of selected indices so that peak tensor sizes never exceed a bound, at the price of repeating smaller contractions; `Cotengra` balances this trade-off automatically. `Quimb` then executes the

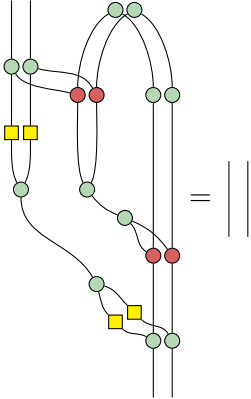


Figure 3: If we double the teleportation protocol diagram from Figure 1, we obtain a ZX diagram which can be converted into a tensor network for evaluation or, for example, to PyZX for simplification. In this example, the diagram can be simplified and is equal to the identity channel on a qubit.

contraction according to the chosen plan, returning either a single tensor or a scalar.

7 Examples

We provide three examples of the use of **Optyx**: simulation of boson sampling with entangled states, distributed entanglement generation, and a variational optimisation scenario.

7.1 Boson sampling with entangled states

This experiment showcases exact classical simulations of quantum photonic circuits using two methods: a permanent-based approach (using a **Perceval** backend) and a tensor network-based approach (**Cotengra**, **Quimb**). Simulations were limited to 350 GB memory and 300 seconds run-time.

Circuits were constructed as layered interferometers with parameterised Mach-Zehnder (MZI) ansätze. For n modes, three depth scalings were used: constant ($l = 2$), logarithmic ($l = \lfloor \log_2(kn) \rfloor$, $k = 7/5$), and linear ($l = \lfloor n/2 + 1 \rfloor$), with layer parameters sampled uniformly from $[0, 1]$. Identical circuits were used for all backends and saved for reproducibility. The entangled states chosen were linear cluster states (dual-rail encoded graph states) implemented in representations compatible with both **Perceval** and **Optyx**. *Monomials of number operators* [49] were used as

observables with a linear scaling of the total degree with the number of photons ($\lfloor 1.5n \rfloor$).

All simulations used a shared pipeline: circuits compiled to tensor networks in **Optyx**, contraction paths optimised by **Cotengra**, and executed with **Quimb**. In **Perceval**, the corresponding unitaries were evaluated using the **NaiveBackend** implementing Ryser’s [38] or Glynn’s [39] algorithms (the choice of which is determined automatically by **Perceval**). For an example of how an observable of a monomial operator is constructed in **Optyx**, see Code Listing 9 in Appendix C.

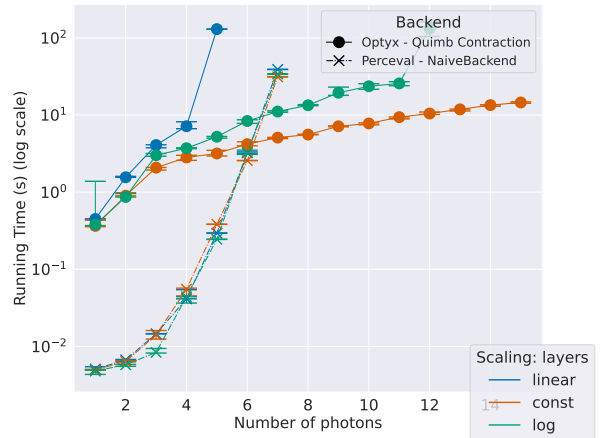


Figure 4: Exact evaluation of boson sampling observables on linear cluster states: we scale the degree of the monomial observable linearly with the number of photons ($\lfloor 1.5n \rfloor$). The depth (number of ansatz layers) is scaled linearly ($l = \lfloor n/2 + 1 \rfloor$), logarithmically ($l = \lfloor \log_2(7n/5) \rfloor$), or kept constant ($l = 2$). Error bars indicate the inter-quantile range (IQR) over 5 random instances.

For entangled inputs (Fig. 4), permanent-based evaluation is fastest on very small circuits (below 6 modes), where its tractability and the overheads of tensor-network methods dominate. As circuit width and monomial degree increase, tensor-network contraction typically overtakes around 6–8 photons, especially for linearly scaling monomials where shared contractions are advantageous. At higher photon numbers, permanent methods often encounter time or memory limits, whereas tensor-network contraction extends the simulable range until large intermediate tensors exhaust memory. In this regime (moderate-high photon number, low depth, entangled sources), tensor-network methods consistently outperform

Ryser/Glynn; nevertheless, both approaches become infeasible at sufficiently large scales. Permanent calculation is largely insensitive to circuit depth, while tensor-network contraction appears less sensitive to circuit width.

Overall, tensor-network methods are preferable for shallow circuits with many photons and entangled inputs. **Optyx** natively supports entangled (e.g., cluster) and hybrid qubit–photon states, which are challenging for permanent-based simulators such as **Perceval**. Preliminary results also indicate that tensor-network methods can offer advantages for observables with feed-forward dependencies, which are difficult to accommodate in permanent-based approaches. Exact tensor network contraction with **Quimb/Cotengra** performs better than permanent-based methods as we increase the photon number and the number of feedforward steps for low-depth circuits (sparse linear optical unitaries). While we focused on exact simulation methods, we expect advantages of tensor network over permanent based evaluation to become more prominent in approximate simulation, see e.g. Ref. [50].

7.2 Distributed entanglement generation

We simulate the effect of partial distinguishability on a distributed setup where entanglement between two remote qubits is mediated by a photonic link. This protocol has been realised experimentally, see e.g. Ref. [1]. In each of the remote nodes, a Bell pair is created between an internal qubit and a dual-rail encoded single-photon. The photons are sent to a central “fusion” station performing a heralded Bell measurement: a specific click pattern projects the remote qubits into an entangled state. Being emitted by different sources, the travelling photons have internal degrees of freedom that make them partially distinguishable and this affects the fidelity of the mediated Bell pair.

To model this setup, we start with two Bell pairs on qubit registers (A_0, A_1) and (A_2, A_3) ,

$$|\Phi^+\rangle = \frac{1}{\sqrt{2}}(|00\rangle + |11\rangle),$$

$$\rho_{\text{in}} = |\Phi^+\rangle\langle\Phi^+|_{A_0A_1} \otimes |\Phi^+\rangle\langle\Phi^+|_{A_2A_3}.$$

The middle qubits A_1, A_2 are dual-rail encoded into photonic modes, each with a two-dimensional internal state. Let $|s_1\rangle, |s_2\rangle$ be unit vectors controlling indistinguishability at fusion.

We bundle the dual-rail encoding, fusion, post-selection onto fusion success and the discarding of the four middle photonic modes (dual-rail-encoded (A_1, A_2)) into $\mathcal{F}_{s_1, s_2}(\rho_{\text{in}})$ which is a heralded fusion map that takes a four-qubit input (on $A_0A_1A_2A_3$) and returns an unnormalized two-qubit state on A_0A_3 :

$$\tilde{\rho}_{\text{out}}(|s_1\rangle, |s_2\rangle) = \mathcal{F}_{s_1, s_2}(\rho_{\text{in}}).$$

From this we report

$$p_{\text{succ}}(|s_1\rangle, |s_2\rangle) = \text{Tr}[\tilde{\rho}_{\text{out}}(|s_1\rangle, |s_2\rangle)],$$

$$\rho_{\text{out}}(|s_1\rangle, |s_2\rangle) = \frac{\tilde{\rho}_{\text{out}}(|s_1\rangle, |s_2\rangle)}{p_{\text{succ}}(|s_1\rangle, |s_2\rangle)},$$

and the fidelity with the Bell target on the surviving pair,

$$F(|s_1\rangle, |s_2\rangle) = \langle\Phi^+| \rho_{\text{out}}(|s_1\rangle, |s_2\rangle) |\Phi^+\rangle.$$

This (given that our target Bell state is a pure state) is equal to the channel fidelity,

$$\mathcal{F}(|\Phi^+\rangle\langle\Phi^+|, \rho_{\text{out}}) = \left(\text{Tr} \sqrt{\sqrt{\rho_{\text{out}}} |\Phi^+\rangle\langle\Phi^+| \sqrt{\rho_{\text{out}}}} \right)^2. \quad (2)$$

In the sweep we fix $|s_1\rangle$ and vary $|s_2\rangle$ so that their overlap $x = \langle s_1 | s_2 \rangle$ ranges from 0 (orthogonal) to 1 (indistinguishable). We plot F versus x : as $x \rightarrow 1$, $F \rightarrow 1$; lowering x smoothly degrades the entanglement after fusion, isolating the role of internal-state overlap (see Figure 5). We give the details of the construction in Appendix D.

7.3 Variational eigensolver

The Bose-Hubbard model is a lattice model for interacting bosons, capturing the competition between tunnelling (t) and on-site repulsion (U) that drives the superfluid-Mott-insulator transition. It provides a quantitatively accurate description of cold atoms in optical lattices [51].

For a graph $G = (V, E)$ with $|V| = N$ sites, the Hamiltonian is

$$H(t, U, \mu) = -t \sum_{\langle i, j \rangle \in E} (a_i^\dagger a_j + a_j^\dagger a_i) + \frac{U}{2} \sum_{i \in V} n_i(n_i - 1) - \mu \sum_{i \in V} n_i, \quad (3)$$

with a_i^\dagger, a_i the creation/annihilation operators and $n_i = a_i^\dagger a_i$. In **Optyx**, we implement these as

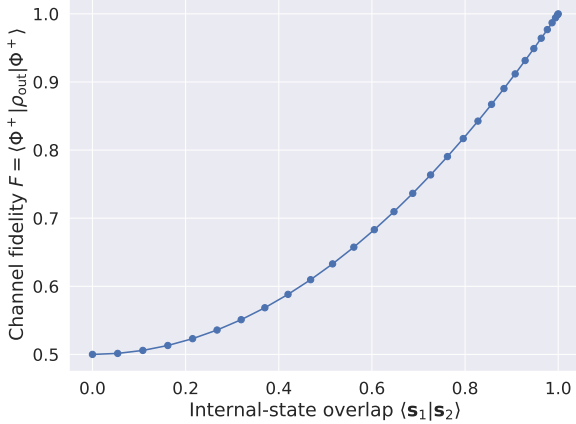


Figure 5: Distributed entanglement generation via photonic fusion with an internal degree of freedom: two Bell pairs are prepared; the middle qubits are dual-rail encoded with internal states $|s_1\rangle$ and $|s_2\rangle$, fused, and we post-select on the standard success outcome. Plotted is the post-selected fidelity $F = \langle \Phi^+ | \rho_{\text{out}} | \Phi^+ \rangle$ (equal to the channel fidelity, given the target state is pure) of the surviving pair (A_0, A_3) versus the internal-state overlap $x = \langle s_1 | s_2 \rangle$. Fidelity approaches 1 for indistinguishable internal states ($x \rightarrow 1$) and decreases smoothly as x is reduced.

photonic channels and assemble H by summing site- and edge-local terms; the resulting channel diagram compiles to a ZX/ZW-based intermediate representation and then to a tensor network.

We prepare a small photonic ansatz $\psi(\theta)$ and evaluate the variational energy $E(\theta) = \langle \psi(\theta) | H | \psi(\theta) \rangle$. The ansatz is based on having three photons in three modes and putting them through a variable-depth MZI circuit. We discard one mode after the MZI ansatz to allow for variable number of photons to enter the Bose-Hubbard Hamiltonian. Energies and gradients are obtained by invoking the backend to produce the corresponding results; in this example we use an exact permanent-based evaluator suitable for small instances (`PermanentBackend`), but the same diagram could compile to more scalable contraction backends. See Figure 6 for an example of gradient descent on a two-site chain. For the construction of the Hamiltonian and the optimisation procedure, see Appendix E.

8 Conclusion and outlook

We introduced `Optyx`, an open-source Python package for the design, simulation, and optimisation of hybrid qubit-photon quantum circuits.

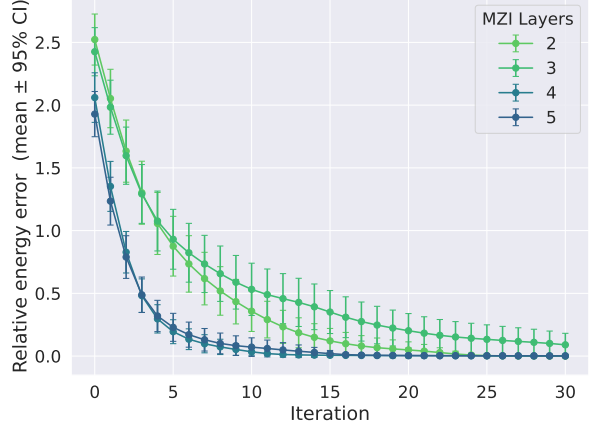


Figure 6: Bose-Hubbard model – variational optimisation: we take a two-site chain with $(t, U, \mu) = (0.10, 4.0, 2.0)$, form the expectation diagram $\langle \psi(\theta) | H | \psi(\theta) \rangle$ for the ansatz $|\psi(\theta)\rangle$, and run gradient descent from a constant initialisation of θ . A learning-rate of 0.001 over 30 steps produces a decrease of the energy in this small instance. 95% Confidence interval (CI) is calculated over 100 different random initialisations. The ansatz is constructed by inputting three photons in three modes and composing them with the varying-depth MZI circuit. We also discard one mode after the ansatz to allow for variable number of photons to enter the Bose-Hubbard Hamiltonian.

The framework provides a categorical semantics in which qubits, bosonic modes, and classical control are represented within a common diagrammatic language, and circuits are evaluated using tensor-network methods. This allows scalable simulation and differentiation of heterogeneous architectures, positioning `Optyx` as a platform for testing new ideas in hybrid and distributed quantum computing. The package has already been used to simulate a number of interesting scenarios. In Ref. [52], the authors numerically simulated a photonic kernel method (a previous version of `Optyx` was used) and benchmarked SVM classification accuracies on synthetic datasets against classical kernels (Gaussian, NTK, polynomial, linear).

In the longer term, we envisage `Optyx` as a tool to probe several directions of current research. In quantum communication, the framework can be extended to model photonic carriers and their interaction with local processors, enabling the study of entanglement distribution, transmission losses, and interface fidelity. For distributed error correction, explicit qubit-photon semantics allow fault-tolerant schemes to be sim-

ulated, and the package can be adapted to facilitate the analysis of resource requirements and threshold behaviour. A tool supporting photonic nodes is needed because in quantum communication protocols, photonic errors cannot always be translated into qubit errors. Compilation for distributed hardware requires mapping abstract circuit descriptions to architectures with limited connectivity and heterogeneous links; **Optyx** can serve as a testbed for developing and benchmarking such strategies. Hybrid architectures also depend critically on light-matter interfaces. By allowing the explicit modelling of conversion processes between photons and stationary excitations, **Optyx** provides a platform for investigating the feasibility and limitations of heterogeneous systems such as ion-photonic hybrids.

On the near-term development side, several extensions are planned. Large-scale hybrid simulations will benefit from approximate tensor-network methods tailored to qubit-boson interactions, such as controlled truncation in **Quimb**, and **Optyx** offers an environment in which to design and benchmark these techniques. Improvements to the user interface and interoperability with external software stacks are also needed, so that circuits can be constructed, simulated, and exported more easily in both theoretical and experimental workflows.

In summary, **Optyx** is not only a categorical and computational framework but also a practical testbed. By extending the package in response to the demands of quantum communication, distributed error correction, compilation, and light-matter interfacing, we aim to make **Optyx** a platform where new ideas can be rapidly prototyped and evaluated against realistic architectural constraints.

Acknowledgements We would like to thank Mark Koch for developing early prototypes which laid the groundwork for **Optyx** and for providing useful feedback on the manuscript. We would also like to thank Michael Lubasch for comments and suggestions on the manuscript.

References

[1] D. Main, P. Drmota, D. P. Nadlinger, E. M. Ainley, A. Agrawal, B. C. Nichol, R. Srinivas, G. Araneda, and D. M. Lucas. “Distributed quantum computing across an optical network link”. *Nature* **638**, 383–388 (2025).

[2] H. Aghaei Rad, T. Ainsworth, R. N. Alexander, B. Altieri, M. F. Askarani, R. Baby, L. Banchi, B. Q. Baragiola, J. E. Bourassa, R. S. Chadwick, I. Charania, H. Chen, M. J. Collins, P. Contu, N. D’Arcy, G. Dauphinais, R. De Prins, D. Deschenes, I. Di Luch, S. Duque, P. Edke, S. E. Fayer, S. Ferracin, H. Ferretti, J. Gefaell, S. Glancy, C. González-Arciniegas, T. Grainge, Z. Han, J. Hastrup, L. G. Helt, T. Hillmann, J. Hundal, S. Izumi, T. Jaeken, M. Jonas, S. Kocsis, I. Krasnokutska, M. V. Larsen, P. Laskowski, F. Laudenbach, J. Lavoie, M. Li, E. Lomonte, C. E. Lopetegui, B. Luey, A. P. Lund, C. Ma, L. S. Madsen, D. H. Mahler, L. Mantilla Calderón, M. Menotti, F. M. Miatto, B. Morrison, P. J. Nadkarni, T. Nakamura, L. Neuhaus, Z. Niu, R. Noro, K. Papirov, A. Pesah, D. S. Phillips, W. N. Plick, T. Rogalsky, F. Rortais, J. Sabines-Chesterking, S. Safavi-Bayat, E. Sazhaev, M. Seymour, K. Rezaei Shad, M. Silverman, S. A. Srinivasan, M. Stephan, Q. Y. Tang, J. F. Tasker, Y. S. Teo, R. B. Then, J. E. Tremblay, I. Tzitrin, V. D. Vaidya, M. Vasmer, Z. Vernon, L. F. S. S. M. Villalobos, B. W. Walshe, R. Weil, X. Xin, X. Yan, Y. Yao, M. Zamani Abnili, and Y. Zhang. “Scaling and networking a modular photonic quantum computer”. *Nature* **638**, 912–919 (2025).

[3] Jiawei Qiu, Yang Liu, Ling Hu, Yukai Wu, Jingjing Niu, Libo Zhang, Wenhui Huang, Yuanzhen Chen, Jian Li, Song Liu, Youpeng Zhong, Luming Duan, and Dapeng Yu. “Deterministic quantum state and gate teleportation between distant superconducting chips”. *Science Bulletin* **70**, 351–358 (2025).

[4] V. Krutyanskiy, M. Galli, V. Krcmarsky, S. Baier, D. A. Fioretto, Y. Pu, A. Mazzloom, P. Sekatski, M. Canteri, M. Teller, J. Schupp, J. Bate, M. Meraner, N. Sanguinetti, B. P. Lanyon, and T. E. Northup. “Entanglement of trapped-ion qubits separated by 230 meters”. *Phys. Rev. Lett.* **130**, 050803 (2023).

[5] Jiu-Peng Chen, Chi Zhang, Yang Liu, Cong Jiang, Wei-Jun Zhang, Zhi-Yong Han, Shi-Zhao Ma, Xiao-Long Hu, Yu-Huai Li, Hui Liu, Fei Zhou, Hai-Feng Jiang, Teng-Yun Chen, Hao Li, Li-Xing You, Zhen Wang, Xiang-Bin Wang, Qiang Zhang, and Jian-Wei Pan. “Twin-field quantum key distribution over a 511 km optical fibre linking two distant metropolitan areas”. *Nature Photonics* **15**, 570–575 (2021).

[6] Ali Javadi-Abhari, Matthew Treinish, Kevin Krsulich, Christopher J. Wood, Jake Lishman, Julien Gacon, Simon Martiel, Paul D. Nation, Lev S. Bishop, Andrew W. Cross, Blake R. Johnson, and Jay M. Gambetta. “Quantum computing with Qiskit” (2024). [arXiv:2405.08810](https://arxiv.org/abs/2405.08810).

[7] Cirq Developers. “Cirq”. *Zenodo*. (2025).

[8] Seyon Sivarajah, Silas Dilkes, Alexander Cowtan, Will Simmons, Alec Edgington, and Ross Duncan. “ $t|ket\rangle$: a retargetable compiler for nisq devices”. *Quantum Science and Technology* **6**, 014003 (2020).

[9] Nathan Killoran, Josh Izaac, Nicolás Quesada, Ville Bergholm, Matthew Amy, and Christian Weedbrook. “Strawberry Fields: A software platform for photonic quantum computing”. *Quantum* **3**, 129 (2019). [arXiv:1804.03159](https://arxiv.org/abs/1804.03159).

[10] Brajesh Gupta, Josh Izaac, and Nicolás Quesada. “The Walrus: a library for the calculation of hafnians, Hermite polynomials and Gaussian boson sampling”. *Journal of Open Source Software* **4**, 1705 (2019).

[11] Nicolas Heurtel, Andreas Fyrillas, Grégoire de Gliniasty, Raphaël Le Bihan, Sébastien Malherbe, Marceau Pailhas, Eric Bertasi, Boris Bourdoncle, Pierre-Emmanuel Emeriau, Rawad Mezher, Luka Music, Nadia Belabas, Benoît Valiron, Pascale Senellart, Shane Mansfield, and Jean Senellart. “Perceval: A Software Platform for Discrete Variable Photonic Quantum Computing”. *Quantum* **7**, 931 (2023).

[12] Javier Osca and Jiri Vala. “Soqcs: A stochastic optical quantum circuit simulator”. *SoftwareX* **25**, 101603 (2024).

[13] Struchalin Gleb and Dyakonov Ivan. “Linopt: a library for linear optics calcu-
lations”. <https://github.com/qotlabs/linopt> (2025).

[14] Zoltán Kolarovszki, Tomasz Rybotycki, Péter Rakyta, Ágoston Kaposi, Boldizsár Poór, Szabolcs Jóczik, Dániel T. R. Nagy, Henrik Varga, Kareem H. El-Safty, Gregory Morse, Michał Oszmaniec, Tamás Kozsik, and Zoltán Zimborás. “Piquasso: A Photonic Quantum Computer Simulation Software Platform”. *Quantum* **9**, 1708 (2025).

[15] Xanadu. “Mr mustard: Your universal differentiable toolkit for quantum optics”. <https://github.com/XanaduAI/MrMustard> (2025).

[16] J.R. Johansson, P.D. Nation, and Franco Nori. “QuTiP: An open-source Python framework for the dynamics of open quantum systems”. *Computer Physics Communications* **183**, 1760–1772 (2012).

[17] Sebastian Krämer, David Plankensteiner, Laurin Ostermann, and Helmut Ritsch. “QuantumOptics.jl: A Julia framework for simulating open quantum systems”. *Computer Physics Communications* **227**, 109–116 (2018).

[18] Jie Lin, Benjamin MacLellan, Sobhan Ghanbari, Julie Belleville, Khuong Tran, Luc Robicaud, Roger G. Melko, Hoi-Kwong Lo, and Piotr Roztocki. “GraphiQ: Quantum circuit design for photonic graph states”. *Quantum* **8**, 1453 (2024).

[19] Shinichi Sunami and Masato Fukushima. “Graphix: optimizing and simulating measurement-based quantum computation on local-Clifford decorated graph” (2022). [arXiv:2212.11975](https://arxiv.org/abs/2212.11975).

[20] Miriam Backens, Hector Miller-Bakewell, Giovanni de Felice, Leo Lobski, and John van de Wetering. “There and back again: A circuit extraction tale”. *Quantum* **5**, 421 (2021).

[21] Ross Duncan, Aleks Kissinger, Simon Perdrix, and John Van De Wetering. “Graph-theoretic Simplification of Quantum Circuits with the ZX-calculus”. *Quantum* **4**, 279 (2020).

[22] Niel de Beaudrap, Xiaoning Bian, and Quanlong Wang. “Fast and Effective Techniques

for T-Count Reduction via Spider Nest Identities”. *LIPICS, Volume 158, TQC 2020* **158**, 11:1–11:23 (2020).

[23] Tom Peham, Lukas Burgholzer, and Robert Wille. “Equivalence Checking of Quantum Circuits With the ZX-Calculus”. *IEEE Journal on Emerging and Selected Topics in Circuits and Systems* **12**, 662–675 (2022).

[24] Ross Duncan and Maxime Lucas. “Verifying the Steane code with Quantomatic”. *Electronic Proceedings in Theoretical Computer Science* **171**, 33–49 (2014).

[25] Aleks Kissinger and John Van De Wetering. “PyZX: Large Scale Automated Diagrammatic Reasoning”. *Electronic Proceedings in Theoretical Computer Science* **318**, 229–241 (2020).

[26] Giovanni De Felice, Alexis Toumi, and Bob Coecke. “DisCoPy: Monoidal Categories in Python”. *Electronic Proceedings in Theoretical Computer Science* **333**, 183–197 (2021).

[27] Changhun Oh, Minzhao Liu, Yuri Alexeev, Bill Fefferman, and Liang Jiang. “Classical algorithm for simulating experimental gaussian boson sampling”. *Nature Physics* **20**, 1461–1468 (2024).

[28] Minzhao Liu, Changhun Oh, Junyu Liu, Liang Jiang, and Yuri Alexeev. “Simulating lossy gaussian boson sampling with matrix-product operators”. *Phys. Rev. A* **108**, 052604 (2023).

[29] Michael L. Wall, Arghavan Safavi-Naini, and Ana Maria Rey. “Simulating generic spin-boson models with matrix product states”. *Phys. Rev. A* **94**, 053637 (2016).

[30] Michael Lubasch, Antonio A. Valido, Jelmer J. Renema, W. Steven Kolthammer, Dieter Jaksch, M. S. Kim, Ian Walmsley, and Raúl García-Patrón. “Tensor network states in time-bin quantum optics”. *Phys. Rev. A* **97**, 062304 (2018).

[31] Florian A. Y. N. Schröder and Alex W. Chin. “Simulating open quantum dynamics with time-dependent variational matrix product states: Towards microscopic correlation of environment dynamics and reduced system evolution”. *Phys. Rev. B* **93**, 075105 (2016).

[32] Giovanni de Felice, Boldizsár Poór, Lia Yeh, Cole Comfort, Mateusz Kupper, William Cashman, and Bob Coecke. “A dataflow programming framework for linear optical distributed quantum computing”. To appear in *Quantum* (2025).

[33] E. Knill, R. Laflamme, and G. J. Milburn. “A scheme for efficient quantum computation with linear optics”. *Nature* **409**, 46–52 (2001).

[34] Bob Coecke and Ross Duncan. “Interacting quantum observables: categorical algebra and diagrammatics”. *New Journal of Physics* **13**, 043016 (2011).

[35] Giovanni de Felice, Razin A. Shaikh, Boldizsár Poór, Lia Yeh, Quanlong Wang, and Bob Coecke. “Light-matter interaction in the zxw calculus”. In Shane Mansfield, Benoît Valiron, and Vladimir Zamdzchiev, editors, *Proceedings of the Twentieth International Conference on Quantum Physics and Logic*, Paris, France, 17-21st July 2023. Volume 384 of *Electronic Proceedings in Theoretical Computer Science*, pages 20–46. Open Publishing Association (2023).

[36] Mark Koch, Alan Lawrence, Kartik Singh, Seyon Sivarajah, and Ross Duncan. “Guppy: pythonic quantum-classical programming”. In *Informal Proceedings of the Fourth International Workshop on Programming Languages for Quantum Computing (PLanQC24)*. (2024). url: <https://ks.cs.uchicago.edu/publication/guppy-planqc>.

[37] L.G. Valiant. “The complexity of computing the permanent”. *Theoretical Computer Science* **8**, 189–201 (1979).

[38] Herbert John Ryser. “Combinatorial mathematics”. Number v. 14 in Carus Mathematical Monographs. Mathematical Association of America; Wiley New York. Buffalo (1963).

[39] David G. Glynn. “The permanent of a square matrix”. *European Journal of Combinatorics* **31**, 1887–1891 (2010).

[40] Scott Aaronson and Travis Hance. “Generalizing and derandomizing Gurvits’s approximation algorithm for the permanent”. *Quantum Info. Comput.* **14**, 541–559 (2014).

[41] Nicolas Heurtel, Shane Mansfield, Jean Senellart, and Benoît Valiron. “Strong simulation of linear optical processes”. *Computer Physics Communications* **291**, 108848 (2023).

[42] Robert Raussendorf. “Measurement-based quantum computation with cluster states”. *International Journal of Quantum Information* **07**, 1053–1203 (2009).

[43] Daniel E. Browne and Terry Rudolph. “Resource-Efficient Linear Optical Quantum Computation”. *Physical Review Letters* **95**, 010501 (2005).

[44] C. K. Hong, Z. Y. Ou, and L. Mandel. “Measurement of subpicosecond time intervals between two photons by interference”. *Physical Review Letters* **59**, 2044–2046 (1987).

[45] Adrian J. Menssen, Alex E. Jones, Benjamin J. Metcalf, Malte C. Tichy, Stefanie Barz, W. Steven Kolthammer, and Ian A. Walmsley. “Distinguishability and many-particle interference”. *Phys. Rev. Lett.* **118**, 153603 (2017).

[46] Daniel Jost Brod and Michał Oszmaniec. “Classical simulation of linear optics subject to nonuniform losses”. *Quantum* **4**, 267 (2020).

[47] Grady Booche, James Rumbaugh, and Ivar Jacobson. “The unified modeling language user guide”. Addison-Wesley. (2005). 2 edition.

[48] Bob Coecke, Chris Heunen, and Aleks Kissinger. “Categories of quantum and classical channels”. *Quantum Information Processing* **15**, 5179–5209 (2016).

[49] Giorgio Facelli, David D. Roberts, Hugo Wallner, Alexander Makarovskiy, Zoë Holmes, and William R. Clements. “Exact gradients for linear optics with single photons” (2024). [arXiv:2409.16369](https://arxiv.org/abs/2409.16369).

[50] Changhun Oh, Kyungjoo Noh, Bill Fefferman, and Liang Jiang. “Classical simulation of lossy boson sampling using matrix product operators”. *Physical Review A* **104**, 022407 (2021).

[51] Matthew P. A. Fisher, Peter B. Weichman, G. Grinstein, and Daniel S. Fisher. “Boson localization and the superfluid-insulator transition”. *Physical Review B* **40**, 546–570 (1989).

[52] Zhenghao Yin, Iris Agresti, Giovanni De Felice, Douglas Brown, Alexis Toumi, Ciro Pentangelo, Simone Piacentini, Andrea Crespi, Francesco Ceccarelli, Roberto Osellame, Bob Coecke, and Philip Walther. “Experimental quantum-enhanced kernel-based machine learning on a photonic processor”. *Nature Photonics* **19**, 1020–1027 (2025).

A Kraus maps and custom channels

`Optyx` provides a way to define custom channels and boxes, which can be used to create new generators. In order to make the new generator simulable using tensor networks, a box inheriting from `core.diagram.Box` must implement the `truncation_specification` method (for the class diagram see Figure 2). This specifies how a box acts on the basis vectors of the input and output edges, and is used to construct a tensor for a given box. Once the box representing a tensor is built, it can be used as a Kraus map for a channel. More details of this are explained in Section 6 and in the documentation of `Optyx`.

```

1  from optyx.core.diagram import Box
2  from optyx.core.channel import Channel
3  from optyx.utils.utils import BasisTransition
4
5  class MyCustomBox(Box):
6      def __init__(self, dom, cod, myparam):
7          super().__init__("MyBox", dom, cod)
8          self.myparam = myparam
9
10     def truncation_specification(
11         self,
12         inp: Tuple[int, ...] = None,

```

```

13     max_output_dims: Tuple[int, ...] = None
14 ) -> Iterable[BasisTransition]:
15     # get output basis_elements
16     # for an input basis element inp
17     for basis_element in basis_elements:
18         # calculate the amplitude
19         yield BasisTransition(
20             out=basis_element,
21             amp=amplitude
22         )
23
24 mychannel = lambda dom, cod, mp: Channel(
25     "MyChannel",
26     MyCustomBox(dom, cod, mp)
27 )

```

Code Listing 7: Template for defining a custom box and channel in Optyx.

B Teleportation using fusion measurements

The example in Code Listing 8 shows how to implement a teleportation protocol using a fusion type II measurement. The protocol uses a Bell pair as a channel to teleport a qubit from one dual-rail encoding to another. The measurement result is used to apply a correction on the teleported qubit. The entire protocol is shown in Figure 7. We can verify that the protocol implements the identity channel (up to a normalisation factor) by evaluating the diagram and comparing it to the identity channel on one dual-rail qubit.

This protocol showcases the seamless integration of classical and quantum resources in a hybrid photon-qubit architecture in Optyx.

```

1 correction = BitControlledGate(
2     HadamardBS() >>
3     (Phase(0.5) @ qmode) >>
4     HadamardBS()
5 )
6
7 channel_bell = (
8     Z(0, 2) @ Scalar(0.5**0.5) >> DualRail(1) @ DualRail(1)
9 )
10
11 teleportation = (
12     DualRail(1) @ channel_bell >>
13     FusionTypeII() @ qmode**2 >>
14     PostselectBit(1) @ correction >>
15     DualRail(1).dagger()
16 )
17
18 array_teleportation = teleportation.eval().tensor.array
19
20 array_id = (
21     Id(1) @ Scalar(0.5**0.5)
22 ).eval().tensor.array
23
24 assert np.allclose(array_teleportation, array_id)

```

Code Listing 8: Teleportation protocol using dual-rail encoding, fusion measurement, and classical control.

C Monomials of number operators

We can create a circuit to evaluate a monomial of number operators in a photonic circuit. This example uses a bosonic product state as input (`Create(1, 1, 1, 1)`) but other states can be considered.

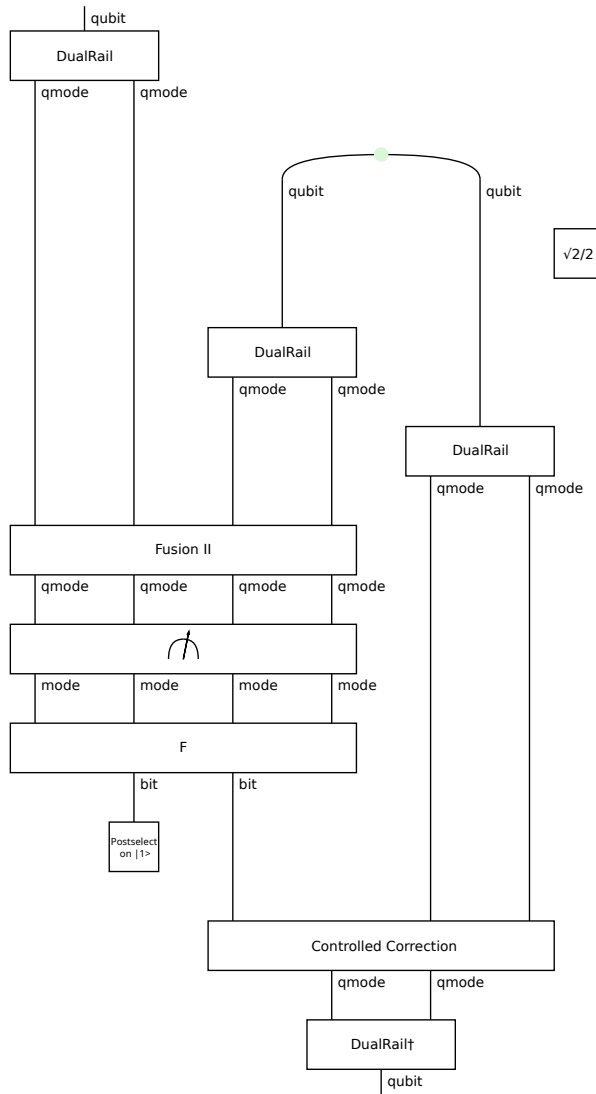


Figure 7: Diagram of the teleportation protocol using a fusion measurement. The protocol demonstrates the transfer of quantum information using entanglement and classical communication.

```

1 from optyx.photonic import (
2     ansatz, NumOp, Create
3 )
4
5 def chip_mzi(w, 1):
6     """Create a random unitary
7     using a rectangular mesh of MZIs."""
8     ansatz_ = ansatz(w, 1)
9     syms = list(ansatz_.free_symbols)
10    s = [(i, np.random.uniform(0, 1))
11          for i in syms]
12    return ansatz_.subs(*s)
13
14 powers = [1, 2, 1, 3]
15 U = chip_mzi(4, 4)
16 monomial_layer = Diagram.tensor(
17     *[[
18         Diagram.then(
19             *[NumOp()] * p
20         ) for p in powers
21     ]]

```

```

22 )
23
24 diagram = (
25     Create(1, 1, 1, 1) >>
26     U >>
27     monomial_layer >>
28     U.dagger() >>
29     Create(1, 1, 1, 1).dagger()
30 )
31
32 result = diagram.eval().tensor

```

Code Listing 9: Builds and evaluates a monomial of number operators in a photonic circuit. A random unitary U is generated by a rectangular MZI mesh `ansatz(w,1)` with uniformly sampled parameters. For powers $\{p_k\}$, the layer implements $\bigotimes_k n_k^{p_k}$ by applying `NumOp()` p_k times on mode k . The diagram computes $\langle \psi | U^\dagger (\bigotimes_k n_k^{p_k}) U | \psi \rangle$.

D Distributed entanglement generation

We simulate fusion-based entanglement generation with an internal degree of freedom (DoF) that controls distinguishability. Two Bell pairs are prepared; the two middle qubits are mapped to dual-rail photonic modes with internal states $|s_1\rangle, |s_2\rangle$. These modes interfere in a fusion primitive and we herald success by post-selecting detector outcomes (1,0). Upon success, the photonic modes are discarded and the two outer qubits remain.

In the sweep, $|s_1\rangle$ is fixed and $|s_2\rangle$ is rotated from parallel to orthogonal, so the overlap $\langle s_1 | s_2 \rangle$ ranges from 1 to 0. For each setting we compute:

- **Numerator (overlap with Bell):** the overlap of the post-selected output with $|\Phi^+\rangle$,

$$F(|s_1\rangle, |s_2\rangle) = \langle \Phi^+ | \tilde{\rho}_{\text{out}}(|s_1\rangle, |s_2\rangle) | \Phi^+ \rangle.$$

- **Denominator (success probability):** the post-selected trace,

$$p_{\text{succ}} = \text{Tr}[\tilde{\rho}_{\text{out}}(|s_1\rangle, |s_2\rangle)].$$

- **Fidelity (conditional on success):**

$$F = \frac{F(|s_1\rangle, |s_2\rangle)}{p_{\text{succ}}} = \langle \Phi^+ | \rho_{\text{out}}(|s_1\rangle, |s_2\rangle) | \Phi^+ \rangle, \quad \rho_{\text{out}} = \frac{\tilde{\rho}_{\text{out}}}{p_{\text{succ}}}.$$

```

1 from optyx.qubits import Z, Scalar, Id, Discard
2 from optyx.photonic import DualRail, FusionTypeII
3 from optyx.classical import PostselectBit
4 from optyx.core.channel import Diagram
5 import numpy as np, math
6 import matplotlib.pyplot as plt
7
8 bell_state = (Z(0, 2) @ Scalar(0.5 ** 0.5))
9 dual_rail_encoding = lambda s: DualRail(1, internal_states=[s])
10 post_select = PostselectBit(1) @ PostselectBit(0)
11
12 def fusion(internal_state_1, internal_state_2):
13     @Diagram.from_callable(dom=0, cod=2)
14     def d():
15         a = (bell_state @ bell_state)()
16         b = (dual_rail_encoding(internal_state_1) @ dual_rail_encoding(
17             internal_state_2))(a[1], a[2])
18         c = FusionTypeII()(*b)
19         post_select(c[0], c[1])

```

```

19     return a[0], a[3]
20
21
22 def rotated_unit_vectors(n=30):
23     for i in range(n):
24         theta = i * (math.pi/2) / (n - 1)
25         yield (math.cos(theta), math.sin(theta))
26
27 internal_state_1 = (1.0, 0.0)
28 unit_vectors = list(rotated_unit_vectors(30))
29
30 xs, Fs = [], []
31 for s2 in unit_vectors:
32     encoding = dual_rail_encoding(internal_state_1) @ dual_rail_encoding(s2)
33     experiment = (bell_state @ bell_state
34                     >> Id(1) @ (encoding >> FusionTypeII() >> post_select) @ Id(1))
35     num = (experiment >> bell_state.dagger()).inflate(2).eval().tensor.array
36     den = (experiment >> Discard(2)).inflate(2).eval().tensor.array
37     xs.append(np.inner(s2, internal_state_1))
38     Fs.append(num / den)

```

Code Listing 10: Distributed entanglement generation via photonic fusion with an internal degree of freedom.

E Bose-Hubbard model

We construct the Bose-Hubbard Hamiltonian as a sum of terms over a register of $N = |V(G)|$ bosonic modes. Given a NetworkX graph $G = (V, E)$ and scalars t, μ, U , the routine `bose_hubbard_from_graph` returns a single `Diagram` H built entirely in function syntax. For every undirected edge $\{i, j\} \in E$ we add the hopping pair $-t(a_i^\dagger a_j + a_j^\dagger a_i)$ by defining `creation_op` on wire i and `annihilation_op` on wire j . For each site $i \in V$ we add the on-site interaction $(U/2) a_i^\dagger a_i^\dagger a_i a_i$ (i.e. $(U/2) n_i(n_i - 1)$ with $n_i = a_i^\dagger a_i$) by composing two creations followed by two annihilations on wire i and multiplying by `Scalar(U/2)`. Finally, we add the chemical potential term $-\mu n_i$ using the provided one-mode number operator `NumOp()` with `Scalar(-mu)`. All contributions are summed into H . See Code Listing 11.

```

1 import networkx as nx
2 from optyx import Diagram, qmode
3 from optyx.photonic import NumOp, Scalar
4 from optyx import Channel
5 from optyx.core.diagram import mode
6 from optyx.core.zw import W, Create, Select
7
8 creation_op = Channel(
9     "a^\dagger",
10    Create(1) @ mode >> W(2).dagger()
11 )
12
13 annihilation_op = Channel(
14     "a",
15     W(2) >> Select(1) @ mode
16 )
17
18 def bose_hubbard_from_graph(graph: nx.Graph, t: float, mu: float, U: float):
19     nodes = sorted(graph.nodes())
20     idx = {u: i for i, u in enumerate(nodes)}
21     N = len(nodes)
22
23     H = None
24
25     # Hopping: -t (a_i^\dagger a_j + a_j^\dagger a_i)
26     for u, v in graph.edges():

```

```

27     i, j = idx[u], idx[v]
28     for src, dst in ((i, j), (j, i)):
29         @Diagram.from_callable(dom=qmode**N, cod=qmode**N)
30         def hop(*in_wires, src=src, dst=dst):
31             out = list(in_wires)
32             out[src] = creation_op(out[src])
33             out[dst] = annihilation_op(out[dst])
34             Scalar(-t)()
35             return tuple(out)
36     H = hop if H is None else (H + hop)
37
38 # On-site: (U/2) a_i^dagger a_i^dagger a_i a_i
39 for u in nodes:
40     i = idx[u]
41     @Diagram.from_callable(dom=qmode**N, cod=qmode**N)
42     def quartic_i(*in_wires, i=i):
43         w = creation_op(creation_op(in_wires[i]))
44         w = annihilation_op(annihilation_op(w))
45         out = list(in_wires); out[i] = w
46         Scalar(U/2)()
47         return tuple(out)
48     H = quartic_i if H is None else (H + quartic_i)
49
50 # Chemical: -I n_i
51 for u in nodes:
52     i = idx[u]
53     @Diagram.from_callable(dom=qmode**N, cod=qmode**N)
54     def n_i(*in_wires, i=i):
55         out = list(in_wires)
56         out[i] = NumOp()(out[i])
57         Scalar(-mu)()
58         return tuple(out)
59     H = n_i if H is None else (H + n_i)
60
61 return H

```

Code Listing 11: Bose-Hubbard model Hamiltonian for a graph.

We use a photonic variational ansatz circuit consisting of three layers of Mach-Zehnder interferometers and post-selection on one mode, as shown in Code Listing 12.

```

1 from optyx import photonic, classical
2
3 circuit = photonic.Create(1, 1, 1) >> photonic.ansatz(3, 4)

```

Code Listing 12: Bose-Hubbard variational ansatz circuit.

We instantiate a two-site chain $G = \text{path_graph}(2)$ with parameters $(t, U, \mu) = (0.10, 4.0, 2.0)$ and construct the Bose-Hubbard Hamiltonian diagram H . Given a defined variational expectation diagram $\text{expectation} = \langle \psi(\boldsymbol{\theta}) | H | \psi(\boldsymbol{\theta}) \rangle$, the code uses the parameters $\boldsymbol{\theta}$ and defines a callable energy $E(\boldsymbol{\theta})$. Gradients are obtained by applying $\text{expectation}.grad(s)$ for each parameter $s \in \boldsymbol{\theta}$ to yield $\nabla E(\boldsymbol{\theta})$.

A simple gradient-descent routine `optimize` initializes $\boldsymbol{\theta}^{(0)} = [2, \dots, 2]$, uses an initial learning rate $\ell_0 = 5$, and runs 12 iterations. Each step updates coordinates,

$$\theta_k \leftarrow \theta_k - \ell (\nabla E(\boldsymbol{\theta}))_k \quad (k = 1, \dots, m).$$

See Code Listing 13.

```

1 import networkx as nx
2 from tqdm import tqdm
3 from optyx.core.backends import PermanentBackend
4
5 graph = nx.path_graph(2) # 2 sites
6 t, U, mu = 0.10, 4.0, 2.0

```

```

7
8 # one extra qmode to allow variable numbers
9 # of photons to enter the circuit of the bose-hubbard Hamiltonian
10 hamiltonian = bose_hubbard_from_graph(graph, t, mu, U) @ qmode
11
12 def to_float(x):
13     if isinstance(x, complex):
14         assert x.imag < 1e-8, x
15         return x.real
16     return x
17
18 free_syms = list(expectation.free_symbols)
19
20 f_exp = lambda xs: to_float(
21     expectation.lambdify(*free_syms)(*xs)
22     .eval(PermanentBackend())
23     .tensor
24     .array
25 )
26
27 def d_f_exp(xs):
28     return [
29         expectation.grad(s).lambdify(*free_syms)(*xs)
30         .eval(PermanentBackend())
31         .tensor
32         .array
33         for s in free_syms
34     ]
35
36 def optimize(x0):
37     x = x0
38     lr = 0.001
39     steps = 30
40
41     xs = []
42     fxs = []
43     dfxs = []
44
45     for _ in tqdm(range(steps)):
46         fx = f_exp(x)
47         dfx = d_f_exp(x)
48
49         xs.append(x[:])
50         fxs.append(fx)
51         dfxs.append(dfx)
52         for i, dfxx in enumerate(dfx):
53             x[i] = to_float(x[i] - lr * dfxx)
54
55     xs.append(x[:])
56     fxs.append(f_exp(x))
57     dfxs.append(d_f_exp(x))
58
59     return xs, fxs, dfxs
60
61
62 xs, fxs, dfxs = optimize([2]*len(free_syms))

```

Code Listing 13: Variational optimisation of a two-site Bose-Hubbard model.